4. 考察

本年度は、電気生理学測定用オペラント実験装置の開発、BPA暴露が乳幼児期における社会性に与える影響の評価、およびBPA暴露の行動影響評価系の提案の3点を目標として研究を展開した。

1）電気生理学測定用オペラント実験装置の開発:
開発が当初の予定よりも遅れたために、BPA暴露マウスのオペラント条件付けおよびオペラント行動時の生理学的測定には至れなかった。しかし、C57BL/6Jマウスによる評価試行では、マウスを本装置上に固定した場合でも、スキナー箱における自由行動下のオペラント条件付けと同様の学習が可能であることが明らかにできた。本装置では、可動式反応レバーに加えて昇降式給水ノズルを採用することによって、マウスのレバー押し反応と飲水反応をミリ秒単位で正確に制御しており、行動データと電気生理学的データをほぼ同じ時間軸上で評価することが可能である。行動データと生理学的データを同時に評価できる本技術は、化学物質の行動影響評価に広く応用出来るものと言える。今後更なるバリデーションを行い、知的財産権の確保・製品化を目指す予定である。

2）BPA暴露が乳幼児期における社会性に与える影響の評価について:
複数のマウスを同時にオープンフィールドに入れ、グループ化の過程を観察する方法を考案した。この方法は極めて簡便でありながら、乳幼児の社会性（特に愛着や親和性に関する情動的な側面）や個体の集団内で示す逸脱的行動（多動など）が高い精度で検出可能である。本研究ではBPA暴露の影響を認めることができなかったが、試験の実施タイミングや観察環境を変化させることによって更なる検出力の向上が期待できる。社会性評価の試験課題は手続きが煩雑なものが多く、乳幼児に適用できるものが少ない。手続きが簡便で自動化も比較的容易と考えられる本課題は、小児毒性の行動モデルとして標準化するに値すると言える。

3）BPA暴露マウスの行動影響評価系の選定の試み：
行動課題の種類は非常に多く、これらを網羅的に検討することは現実的ではない。そこで本研究では、BPA暴露の行動影響について報告している先行研究の結果を多変量解析によって評価・分類を行うことによって、BPA暴露の認知・情動行動に対する影響評価を効率的に行うことができる行動試験バッテリを提案することを目標とした。分析対象とした資料で用いられた行動試験は27種類・カテゴリに達し、マウス行動解析課題のほぼ全般に渡っていた。しかし、最終的に評価項目（カテゴリ）として有効と考えられた試験は8課題（カテゴリ）であった（スライド11, 12）。更にこの8課題（カテゴリ）の中で、性衝動や動因水準の影響を受けやすい試験課題（非攻撃性社会行動: non-aggressive social behavior、性行動: inter-sexual behavior）およびその他本研究においては採用頻度が低くカテゴリ化が困難であった試験課題（other behavior: rota rod, mirror maze, etc）を除外すると、オープンフィールド・明暗箱試験・高架式十字迷路試験・新奇性試験および空間記憶学習試験の5試験課題がグループ化された。この結果はこれらの試験課題がBPA暴露による認知情動行動影響を適正に評価し得る試験課題群であることを示すものと言える。本研究班の研究においても、上記5課題でBPA暴露の影響が認められていることから、化学物質暴露による認知情動行動影響の評価には、これらの試験課題を含めることが望ましいと考えられる。

5. 結論

本年度の研究では、行動と生理学的評価を同時に行える実験系を開発し、また乳幼児における社会行動の評価系を考案した。標準化のために今後更なる試験の信頼性と妥当性の検討が必要である。また、先行研究および本研究班の研究から、化学物質暴露の認知情動行動影響の評価系にはオープンフィールド・明暗箱試験・高架式十字迷路試験・新奇性試験および空間記憶学習試験を含めることが望ましいことが示された。

別紙４

雑誌

発表者氏名	論文タイトル名	発表誌名	巻号	ページ	出版年
Kondoh S, Inoue K, Igarashi K, Sugizaki H, Shirode-Fukuda Y, Inoue E, Yu T, Takeuchi JK, Kanno J, Bonewald LF, Imai Y.	Estrogen receptor α in osteocytes regulates trabecular bone formation in female mice.	*Bone.*	60	68-77	2013
Higuchi H, Ito E, Iwano H, Oikawa S, Nagahata H.	Effects of vitamin E supplementation on cellular α-tocopherol concentrations of neutrophils in Holstein calves.	Can J Vet Res.	77	120-125	2013
Kanno J, Aisaki K, Igarashi K, Kitajima S, Matsuda N, Morita K, Tsuji M, Moriyama N, Furukawa Y, Otsuka M, Tachihara E, Nakatsu N, Kodama Y.	Oral administration of pentachlorophenol induces interferon signaling mRNAs in C57BL/6 male mouse liver.	*J Toxicol Sci.* 2013;38(4):643-54.	38	643-654	2013
Tominaga T and Tominaga Y.	A new non-scanning confocal microscopy module for functional voltage- sensitive dye and Ca2+ imaging of neuronal circuit activity	Journal of Neurophysiology	110	553-561	2013
Terashita Y, Yamagata K, Tokoro M, Itoi F, Wakayama S, Li C, Sato E, Tanemura K, Wakayama T.	Latrunculin a treatment prevents abnormal chromosome segregation for successful development of cloned embryos.	PLoS One.	24;8 (10)	e78380.	2013

Kogasaka Y, Hoshino Y, Hiradate Y, Tanemura K, Sato E.	Distribution and association of mTOR with its cofactors, raptor and rictor, in cumulus cells and oocytes during meiotic maturation in mice.	Mol Reprod Dev.	80	334-348	2013
Hiraga K, Hoshino Y, Tanemura K, Sato E.	Selection of in vitro-matured porcine oocytes based on localization patterns of lipid droplets to evaluate developmental competence.	J Reprod Dev.	59	405-408	2013
Tominaga T and Tominaga Y.	A new non-scanning confocal microscopy module for functional voltage- sensitive dye and Ca2+ imaging of neuronal circuit activity	Journal of Neurophysiology	110	553-561	2013
Takashi Tominaga, Riichi Kajiwara, and Yoko Tominaga	VSD imaging method of ex vivo brain preparation	Journal of Neuroscience and Neuroengineering	2	211-219	2013
Yi S.H., He X.B., Rhee Y.H., Park C.H., Takizawa T., Nakashima K. & Lee S.H.	Foxa2 acts as a co-activator potentiating expression of the Nurr1-induced DA phenotype via epigenetic regulation.	*Development*	141	761-772	2014
Uesaka M., Nishimura O., Go Y., Nakashima K., Agata K. & Imamura T.	Bidirectional promoters are the major source of gene activation-associated non-coding RNAs in mammals.	*BMC Genomics*	15	35	2014
Yuniarti N., Juliandi B., Muhchyi C., Noguchi H., Sanosaka T. & Nakashima K.	Prenatal exposure to suberoylanilide hydroxamic acid perturbs corticogenesis.	*Neurosci Res*	77	42-49	2013

Urayama S., Semi K., Sanosaka T., Hori Y., Namihira M., Kohyama J., Takizawa T. & Nakashima K.	Chromatin accessibility at a STAT3 target site is altered prior to astrocyte differentiation.	*Cell Struct Funct*	38	55-66	2013
Namhira M. & Nakashima K.	Mechanisms of astrocytogenesis in the mammalian brain.	*Curr Opin Neurobiol*	23	921-927	2013
MuhChyi C., Juliandi B., Matsuda T. & Nakashima K.	Epigenetic regulation of neural stem cell fate during corticogenesis.	*Int J Dev Neurosci*	31	424-433	2013
K. Nose-Ishibashi, J. Watahiki, K. Yamada, M. Maekawa, A. Watanabe, G. Yamamoto, A. Enomoto, Y. Matsuba, T. Nampo, T. Taguchi, Y. Ichikawa, T. C. Saido, K. Mishima, Y. Yamaguchi, T. Yoshikawa, K. Maki.	Soft-diet feeding after weaning affects behavior in mice: potential increase in vulnerability to mental disorders.	Neuroscience	263	257-268	2014
S. Ito, I. Ogiwara, K. Yamada, H. Miyamoto, T. K. Hensch, M. Osawa, K. Yamakawa.	Mouse with Nal.1 haploinsufficiency, a model for Dravet syndrome, exhibits lowered sociability and learning impairment.	Neurobiol. Disease	49	29-40	2013
M. Kabayama, K. Sakoori, K. Yamada, V. G. Ornthanalai, M. Ota, N. Morimura, K. Katayama, N. P. Murphy, J. Aruga.	Rines E3 ubiquitin ligase regulates MAO-A levels and emotional responses.	J. Neurosci.	33	12940-12953	2013

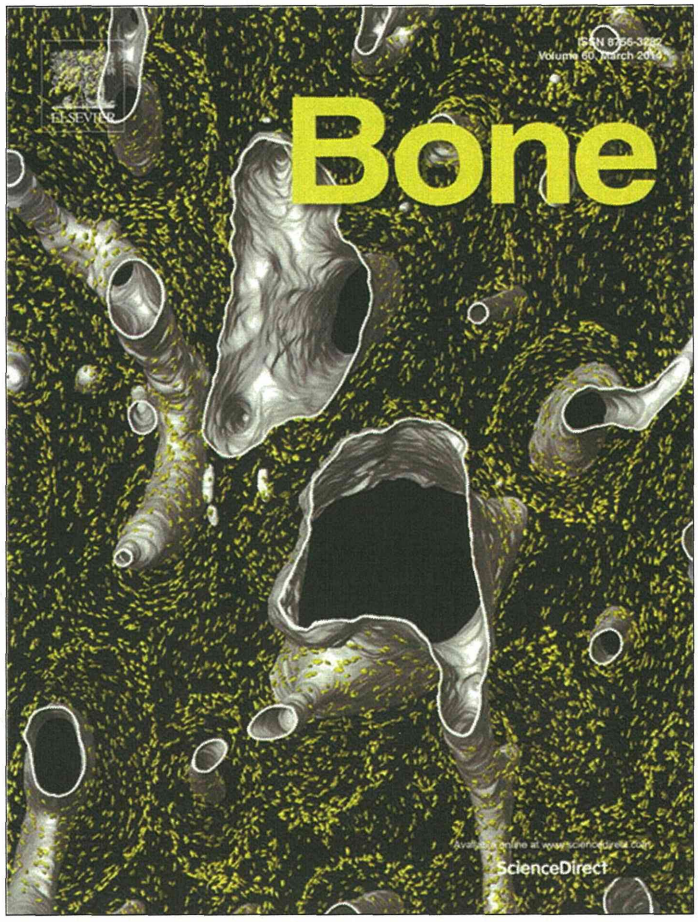

Bone 60 (2014) 68–77

Contents lists available at ScienceDirect

Bone

journal homepage: www.elsevier.com/locate/bone

Original Full Length Article

Estrogen receptor α in osteocytes regulates trabecular bone formation in female mice

Shino Kondoh [a], Kazuki Inoue [a,b,c], Katsuhide Igarashi [d], Hiroe Sugizaki [e], Yuko Shirode-Fukuda [a], Erina Inoue [a], Taiyong Yu [a,b], Jun K. Takeuchi [e,f], Jun Kanno [d], Lynda F. Bonewald [g], Yuuki Imai [a,b,*]

[a] Laboratory of Epigenetic Skeletal Diseases, Institute of Molecular and Cellular Biosciences, The University of Tokyo, Tokyo, Japan
[b] Division of Integrative Pathophysiology, Proteo-Science Center, Graduate School of Medicine, Ehime University, Ehime, Japan
[c] Department of Biological Resources, Integrated Center for Science, Ehime University, Ehime, Japan
[d] Division of Cellular & Molecular Toxicology, Biological Safety Research Center, National Institute of Health Sciences, Tokyo, Japan
[e] Division of Cardiovascular Regeneration, Institute of Molecular and Cellular Biosciences, The University of Tokyo, Tokyo, Japan
[f] JST PRESTO, Japan
[g] Department of Oral Biology, School of Dentistry, University of Missouri at Kansas City, Kansas City, MO, USA

ARTICLE INFO

Article history:
Received 8 July 2013
Revised 26 November 2013
Accepted 4 December 2013
Available online 10 December 2013

Edited by: Shu Takeda

Keywords:
Estrogen
Estrogen receptor α
Osteocyte
Bone formation
Wnt signaling

ABSTRACT

Estrogens are well known steroid hormones necessary to maintain bone health. In addition, mechanical loading, in which estrogen signaling may intersect with the Wnt/β-catenin pathway, is essential for bone maintenance. As osteocytes are known as the major mechanosensory cells embedded in mineralized bone matrix, osteocyte ERα deletion mice ($ER\alpha^{\Delta Ocy/\Delta Ocy}$) were generated by mating ERα floxed mice with Dmp1-Cre mice to determine the role of ERα in osteocytes. Trabecular bone mineral density of female, but not male $ER\alpha^{\Delta Ocy/\Delta Ocy}$ mice was significantly decreased. Bone formation parameters in $ER\alpha^{\Delta Ocy/\Delta Ocy}$ were significantly decreased while osteoclast parameters were unchanged. This suggests that ERα in osteocytes exerts osteoprotective function by positively controlling bone formation. To identify potential targets of ERα, gene array analysis of Dmp1-GFP osteocytes sorted by FACS from $ER\alpha^{\Delta Ocy/\Delta Ocy}$ and control mice was performed. Gene expression microarray followed by gene ontology analyses revealed that osteocytes from $ER\alpha^{\Delta Ocy/\Delta Ocy}$ highly expressed genes categorized in 'Secreted' when compared to control osteocytes. Among them, expression of Mdk and Sostdc1, both of which are Wnt inhibitors, was significantly increased without alteration of expression of the mature osteocyte markers such as Sost and β-catenin. Moreover, hindlimb suspension experiments showed that trabecular bone loss due to unloading was greater in $ER\alpha^{\Delta Ocy/\Delta Ocy}$ mice without cortical bone loss. These data suggest that ERα in osteocytes has osteoprotective functions in trabecular bone formation through regulating expression of Wnt antagonists, but conversely plays a negative role in cortical bone loss due to unloading.

Published by Elsevier Inc.

Introduction

Estrogens clearly maintain physiological homeostasis through the development of reproductive organs and the mammary gland, potentiation of muscles, and through osteoprotection. The osteoprotective actions of estrogens are clearly demonstrated by post-menopausal osteoporosis [1]. The effects of sex steroid hormones on bone tissue can be considered as the combination or sum of the direct effects on bone cells and the indirect effects on other tissues [2]. The indirect effects of estrogen on bone through other tissues have been well described, such as modulation of cytokine production by immune cells and the increased induction of pituitary gland hormones [3,4]. However, the direct effect of estrogens on bone tissue is not fully understood.

Estrogens exert their effects by binding to their own nuclear receptors, such as Estrogen Receptor (ER) α and β, which also function as transcription factors. The conventional ERα null mouse model could not be used to address the direct functions of the receptor in bone due to hormonal imbalance and endocrine disturbances [5–7]. Therefore, the generation and analyses of bone cell type specific deletion is required to clarify the functions of ERα in bone.

Osteoclastic ERα null mice were generated showing that osteoclastic ERα shortens the life span of osteoclasts by promoting apoptosis [8,9]. Ovariectomy can induce osteocyte apoptosis [10] and conventional ERα null mice do not increase bone mass in response to anabolic mechanical loading [11]. Moreover, various groups reported murine skeletal phenotype due to ERα deletion in cells of the osteoblast lineage, suggesting ERα in osteoblastic lineage cells could play important roles in the maintenance of bone metabolism [12–15]. Recently, Windahl

* Corresponding author at: Division of Integrative Pathophysiology, Proteo-Science Center, Graduate School of Medicine, Ehime University, Shitsukawa, Toon, Ehime 791-0295, Japan. Tel.: +81 89 960 5925; fax: +81 89 960 5953.
E-mail address: y-imai@m.ehime-u.ac.jp (Y. Imai).

8756-3282/$ – see front matter. Published by Elsevier Inc.
http://dx.doi.org/10.1016/j.bone.2013.12.005

et al. [13] reported that ERα in osteocytes regulates trabecular bone formation and thus trabecular bone volume in male mice. These results are in contrast to our own findings showing that the precise molecular functions and target genes of ERα in osteocytes still remain elusive.

Osteocytes are embedded in the extracellular matrix of bone and represents more than 90% of the cells existing in bone. Osteocytes possess dendrites that extend throughout the bone and are used to communicate with each other and also with osteoblasts and osteoclasts on the surface of the bone. The function of osteocytes as mechanosensory cells is inferred from their shape and location [16]. In fact, mechanical loading and unloading change osteocyte gene expression *in vivo*, indicating that osteocyte function is affected by loading conditions [17–20]. In addition, they are known to be involved in mineral metabolism through expression of proteins such as FGF23, Phex, Mepe, and Dmp1 [21–24] (for review, see [25]). Recently, it has been postulated that osteocytes can orchestrate skeletal homeostasis through mineral metabolism as well as the regulation of osteoblastic bone formation and osteoclastic bone resorption by secretory proteins such as sclerostin and FGF23. Osteocytes are also reported to regulate osteoblastic bone formation through IGF-1, TGFβ, NO, PGE_2 and sclerostin and to regulate osteoclastic bone resorption through TGFβ, NO, and PGE_2, and RANKL/OPG [26].

Bone mass can be maintained by mechanical loading while unloading or immobilization decreases bone mass. *In vivo* unloading rodent models such as tail suspension can induce bone loss in hind limbs [27] and mechanical loading can increase bone mass in forelimbs [28]. The regulation of bone mass by mechanical loading is mediated, at least in part, through β-catenin signaling [29–31], and estrogen/ER signaling might also be involved in this mechanism [32].

In this study, we examined the functions of ERα in osteocytes by generating mice lacking ERα in osteocytes and analyzing osteocyte gene expression profiles and subjecting them to hindlimb unloading.

Materials and methods

Animals

The ERα floxed mutant ($ER\alpha^{L2/L2}$) mice kindly provided by Dr. Chambon and null alleles with a C57BL/6 J background have been previously described [5]. $ER\alpha^{L2/L2}$ mice were crossed with $Dmp1^{Cre}$ mice [33] to generate $Dmp1^{Cre}$; $ER\alpha^{L2/+}$ mice, and $Dmp1^{Cre}$; $ER\alpha^{L2/L2}$ ($ER\alpha^{\Delta Ocy/\Delta Ocy}$) and $ER\alpha^{L2/L2}$ ($ER\alpha^{flox/flox}$) were obtained by crossing $Dmp1^{Cre}$; $ER\alpha^{L2/+}$ and $ER\alpha^{L2/L2}$. *Dmp1-GFP* mice were kindly provided by Dr. Ivo Kalajzic [34]. All mice were housed in a specific-pathogen-free facility under climate-controlled conditions with a 12-hour light/dark cycle and were provided with water and standard diet (CE-2, CLEA, Japan) *ad libitum*. All animals were maintained and examined according to the protocol approved by the Animal Care and Use Committee of the University of Tokyo.

Genome DNA extraction and cell culture

Various tissues (0.5 g) from $ER\alpha^{\Delta Ocy/\Delta Ocy}$ were harvested, washed with PBS and lysed in 2 ml of lysis buffer with proteinase K (150 μg/ml) overnight. Also, DNA of osteocytes was isolated from the calvariae of $ER\alpha^{\Delta Ocy/\Delta Ocy}$ in which cells on the surface of the bone such as osteoclasts and osteoblasts were removed by sequential enzymatic treatment. Primary osteoblasts obtained from the neonatal calvariae were cultured in αMEM (Life Technologies) containing 10% FBS (Cell Culture Bioscience), 50 μg/ml ascorbic acid (Sigma-Aldrich) and 10 nM β-glycerophosphate (Sigma-Aldrich) for 21 days. Cells were cultured with phenol red free media 24 h before cells were treated with 17β-estradiol. Primary osteoclasts were differentiated from the bone marrow obtained from 6-week-old $ER\alpha^{\Delta Ocy/\Delta Ocy}$ mice using 10 ng/ml of M-CSF (R&D Systems) and 234 ng/ml of GST-RANKL (Oriental Yeast) for 5 days. The genomic DNA was extracted using phenol/chloroform and isopropanol precipitation.

ELISAs

Enzyme-linked Immunoassays, ELISAs, were was performed following the protocols of the Estradiol EIA Kit (Cayman Chemical Company) for estradiol, Testosterone EIA Kit (Cayman Chemical Company) for testosterone, and Rodent Luteinizing Hormone (LH) ELISA TEST (Endocrine Technologies) for LH.

Bone analyses

The BMD of femurs and tibiae obtained from 12-week-old littermates were measured by DXA using a bone mineral analyzer (DCS-600EX: ALOKA). Micro Computed Tomography scanning of the tibiae and femurs was performed using a Scanco Medical μCT35 System (SCANCO Medical) with an isotropic voxel size of 6 μm for trabecular analyses and 12 μm for cortical analyses according to the manufacturer's instructions and the recent guidelines of the American Society for Bone and Mineral Research (ASBMR) [35]. For bone histomorphometry, the mice were double-labeled with intra-peritoneal injections of 16 mg/kg of calcein (Sigma) at 5 and 2 days before sacrifice. Lumbar vertebral bodies were removed from each mouse and fixed with 4% PFA in PBS overnight. Lumbar vertebrae were embedded with MMA after dehydration and the plastic sections were cut by a standard microtome (LEICA) into 7 μm for von Kossa staining and 4 μm for TRAP and Toluidine-blue staining. The region of interest was the secondary spongiosa of L3 and L4. Sections were used for analyses when the bases of the bilateral transverse processes were opened. The region of interest (ROI) in the lumbar vertebral body is the secondary spongiosa, which is separated from the primary spongiosa, cranial and caudal growth plate, according to the same protocol as previously performed [8,36]. Histomorphometric analyses were performed using OsteoMeasure (OsteoMetrics, Inc., GA, USA) according to the ASBMR guideline [37].

Isolation of Dmp1-GFP positive osteocytes by FACS

A highly purified population of osteocytes was isolated from neonatal calvariae by FACS using a modified version of the protocol of Paic F et al. [38]. Cells were isolated from 10-day-old fetal mice calvariae of $ER\alpha^{\Delta Ocy/\Delta Ocy}$ and $ER\alpha^{flox/flox}$ also expressing *Dmp1-GFP*. After removal of the sutures, pooled calvarial tissue was subjected to six sequential, 30-minute digestions in a mixture containing 0.05%/0.2 mM trypsin/EDTA and 1.5 U/ml collagenase-P (Roche) at 37 °C. Cell fractions 4 to 6 were collected, pooled, and re-suspended in Dulbecco's modified Eagle's medium (DMEM, Life Technologies) containing 10% FBS (Hyclone) and centrifuged. Cells were rinsed with PBS and re-suspended in PBS/2% FBS and filtered through a 70-μm filter. Cell sorting was performed using a BD FACS Aria cell sorter. The gate for collecting GFP+ cells was set as GFP+ population to represent 10% to 15% of the total cells in GFP+ mice and 0.8% to 1.0% of total cells in GFP− mice (negative control). GFP+ cells were collected in a tube with 500 μl of PBS/3% FBS.

Gene expression microarray

Gene expression microarray was generated using total RNA extracted from the isolated GFP+ osteocytes of $ER\alpha^{\Delta Ocy/\Delta Ocy}$ and $ER\alpha^{flox/flox}$ as previously described [8] and RNA samples were evaluated using the Affymetrix Mouse Genome 430 2.0 Array following standard Affymetrix protocols (GEO: GSE41997). Gene ontology analyses were performed using DAVID Bioinformatics Resources 6.7 [39].

RNA extraction and RT-qPCR

Total RNA from the pulverized femurs or sorted cells was extracted using TRIZOL (Invitrogen) and RNeasy purification kit (QIAGEN). First-strand cDNA was synthesized from total RNA using PrimeScript RT Master Mix (TaKaRa) and subjected to RT-qPCR using SYBR Premix Ex Taq II

(TaKaRa) or KAPA SYBR Fast qPCR Kits (KAPA Biosystems) with Thermal Cycler Dice (TaKaRa) according to the manufacturer's instructions. Primers were purchased from Takara Bio Inc. (Otsu, Japan) or Operon Biotechnologies (Tokyo, Japan) [8]. Gene expression levels were normalized by *Gapdh* or *Rplp0*. Primer sequences were as follow; *Rplp0*: F 5′-TTCCAGGCTTTGGGCATCA-3′ and R 5′-ATGTTCAGCATGTTCAGCAG TGTG-3′, *Gapdh*: F 5′-AAATGGTGAAGGTCGGTGTG-3′ and R 5′-TGAA GGGGTCGTTGATGG-3′, *ERα*: F 5′-CATGGTCATGGTAAGTGGCA-3′ and R 5′-TCTCTGGGCGACATTCTTCT-3′, *Dmp1*: F 5′-TGAAGAGAGGACGGGT GATT-3′ and R 5′-TCCGTGTGGTCACTATTTGC-3′, *Kera*: F 5′-TGGGATGT CCACGACGACTT-3′ and R 5′-AAGGCAGTAGGGAAACTGGGA-3′, *Mdk*: F 5′-TGCAGCCGACTGCAAATACAA-3′ and R 5′-GGCTTAGTCACGCGGA TGG-3′, *Sostdc1*: F 5′-AAATGTATTTGGTGGACCGC-3′ and R 5′-GAATCA AGCCAGGAATGGAG-3′.

Tail suspension

Tail suspension experiments were performed for female $ERα^{ΔOcy/ΔOcy}$ and $ERα^{flox/flox}$ mice for 4 weeks starting at 8 weeks of age according to previous reports [40,41]. Briefly, a stainless steel harness was superglued to the sides of the tail. Female $ERα^{ΔOcy/ΔOcy}$ and $ERα^{flox/flox}$ mice were then suspended from an eye bolt which was secured into the bars of the top of the rat cage. The animal could rotate 360° with the fish swivel and could also move backwards and forwards about 7.5 cm. Water was provided through a standard water bottle with an extra long angled sipper tube to allow the animals to reach the water. Control female $ERα^{ΔOcy/ΔOcy}$ and $ERα^{flox/flox}$ mice were chained to the cage top during the same period of time, but were allowed to load their hindlimbs to minimize the difference in stress-related effects between the tail-suspended groups and the control groups ($n = 6$ per group).

Statistical analysis

Data were analyzed by a two-tailed student's *t*-test or one-way analysis of variance (ANOVA) to initially determine whether an overall statistically significant change existed before using Tukey's *post hoc* test. For all graphs, data are represented as mean ± SEM. A *p*-value less than 0.05 was considered statistically significant.

Results

Generation of osteocytic ERα deletion mice

To investigate the function of ERα in osteocytes, we generated mice lacking ERα in late-osteoblasts/osteocytes by crossing ERα floxed mice with Dmp1-Cre mice, which express Cre recombinase driven by the Dmp1 promoter. The mice harboring the genotypes of $Dmp1^{Cre}$; $ERα^{L2/L2}$ and $ERα^{L2/L2}$ were analyzed as $ERα^{ΔOcy/ΔOcy}$ and $ERα^{flox/flox}$, respectively. First, to assess cell type specificity of the deletion of the ERα gene locus by Dmp1 promoter-driven Cre recombinase, genomic PCR was performed using DNA extracted from $ERα^{ΔOcy/ΔOcy}$. As a result, a relatively specific deletion of ERα in osteocytes, which were isolated by sequential enzymatic digestion, was detected as an L-band, which was seen only in osteocytes and not in primary cultured osteoblasts or osteoclasts (Fig. 1A). In addition, the ERα mRNA level was examined by qPCR using RNA extracted from femoral bones and GFP-mediated FACS sorted osteocytes of $ERα^{ΔOcy/ΔOcy}$ and $ERα^{flox/flox}$ mice. As a result, there was an approximately 30% and 90% reduction of ERα expression in whole bone and osteocytes, respectively, in $ERα^{ΔOcy/ΔOcy}$ compared to $ERα^{flox/flox}$ mice (Fig. 1B). This significant but low percent deletion in whole bone might reflect ERα expression by other cell types, which are present in the intact femur even though the bone marrow was removed. Also, one group reported that clear deletion of the target gene was detected at the genome level but not the mRNA level when using the Dmp1-Cre mice [42]. Next, body weight was measured every other week from 3 to 12 weeks old. There was no significant difference in body weight between $ERα^{ΔOcy/ΔOcy}$ and $ERα^{flox/flox}$, whereas it was previously reported that ERα total KO mice exhibited a significant increase in body weight [43] (Fig. 1C). Next, we asked if these mice could be a suitable model for analyzing ERα function without the systemic influence of hormones (endocrine disturbances) as described in the conventional ERα null mouse, by examining the concentration of sex steroid hormones. Serum estradiol, testosterone and luteinizing hormone concentrations were measured by ELISA, showing that there were no significant differences between the 12-week-old $ERα^{ΔOcy/ΔOcy}$ and $ERα^{flox/flox}$, regardless of gender (Fig. 1D). Since $ERα^{ΔOcy/ΔOcy}$ mice exhibited a relatively specific deletion of ERα in osteocytes and normal serum sex steroid hormone levels, we concluded that $ERα^{ΔOcy/ΔOcy}$ could be used for analysis of ERα function in osteocytes without the complications of endocrine disturbances.

Osteocytic ERα deletion female mice exhibit an osteopenic phenotype

The BMD of 12-week-old $ERα^{ΔOcy/ΔOcy}$ and $ERα^{flox/flox}$ were measured by DXA, showing that the BMD of female $ERα^{ΔOcy/ΔOcy}$ was significantly decreased in the proximal, not in middle and distal, tibiae compared to that of female $ERα^{flox/flox}$ (Fig. 1E). However, the BMD of tibiae from male $ERα^{ΔOcy/ΔOcy}$ were not significantly different from that of male $ERα^{flox/flox}$ (Fig. 1E). Next, to assess changes in bone structure between female $ERα^{ΔOcy/ΔOcy}$ and $ERα^{flox/flox}$ mice, μCT analysis was performed. Decreased trabecular bone mass in $ERα^{ΔOcy/ΔOcy}$ mice was observed by μCT analysis (Fig. 2A). Trabecular bone of female $ERα^{ΔOcy/ΔOcy}$ exhibited a significant decrease in BV/TV, vBMD, Tb.N and Conn-D, and an increase in Tb.Sp and SMI compared to those of female $ERα^{flox/flox}$ (Fig. 2B). The parameters in metaphyseal cortical bone of female $ERα^{ΔOcy/ΔOcy}$ were not significantly different from that of female $ERα^{flox/flox}$ (Fig. 2C).

Osteocytic ERα regulates bone formation through control of osteoblasts

To examine whether the reduced bone phenotype of $ERα^{ΔOcy/ΔOcy}$ could be caused by alterations in the potential interaction between osteocytes and either osteoblasts or osteoclasts, bone histomorphometry was performed. The number and/or activity of osteoblasts/osteoclasts were examined in $ERα^{ΔOcy/ΔOcy}$ and $ERα^{flox/flox}$, using lumbar vertebrae of 12-week-old female $ERα^{ΔOcy/ΔOcy}$ and $ERα^{flox/flox}$. Parameters related to osteoblastic bone formation, such as N.Ob/B.Pm and Ob.S/BS, were significantly decreased in $ERα^{ΔOcy/ΔOcy}$ compared to $ERα^{flox/flox}$ (Fig. 3). In addition, N.Ocy/B.Ar was also decreased in $ERα^{ΔOcy/ΔOcy}$, which might be due to a decreased number of osteoblasts, which are precursors of osteocytes. Also, the reduction of BFR/BS and MAR in $ERα^{ΔOcy/ΔOcy}$ tended to be significant ($p = 0.07$), due to the reduction of osteoblastic parameters. On the other hand, parameters related to osteoclastic bone resorption, such as N.Oc/B.Pm and Oc.S/BS, were not altered in $ERα^{ΔOcy/ΔOcy}$ when compared to $ERα^{flox/flox}$ (Fig. 3). These results suggested that deficiency of ERα in osteocytes could decrease the number of osteoblasts and consequently their bone forming activity, indicating that bone mass reduction in $ERα^{ΔOcy/ΔOcy}$ could be caused by a reduction of osteoblastic bone formation, not a promotion of osteoclastic bone resorption. In addition, this result implies that osteocytic ERα might positively regulate osteoblastic bone formation by signaling from osteocytes, such as in a paracrine manner or by cell–cell contact.

Gene expression profiles of osteocytes lacking ERα

To determine what secretory proteins or signaling pathways *ERα* may utilize in osteocytes, a gene array analysis of Dmp1-GFP-positive cells from controls and mice with a targeted deletion of *ERα* in osteocytes was performed. Dmp1-GFP mice were crossed with $Dmp1^{Tg/0}$; $ERα^{L2/L2}$ mice to generate *Dmp1-GFP+*; $Dmp1^{Tg/0}$; $ERα^{L2/+}$ mice, and then *Dmp1-GFP+*; $Dmp1^{Tg/0}$; $ERα^{L2/L2}$ (*Dmp1-GFP+*; $ERα^{ΔOcy/ΔOcy}$) and

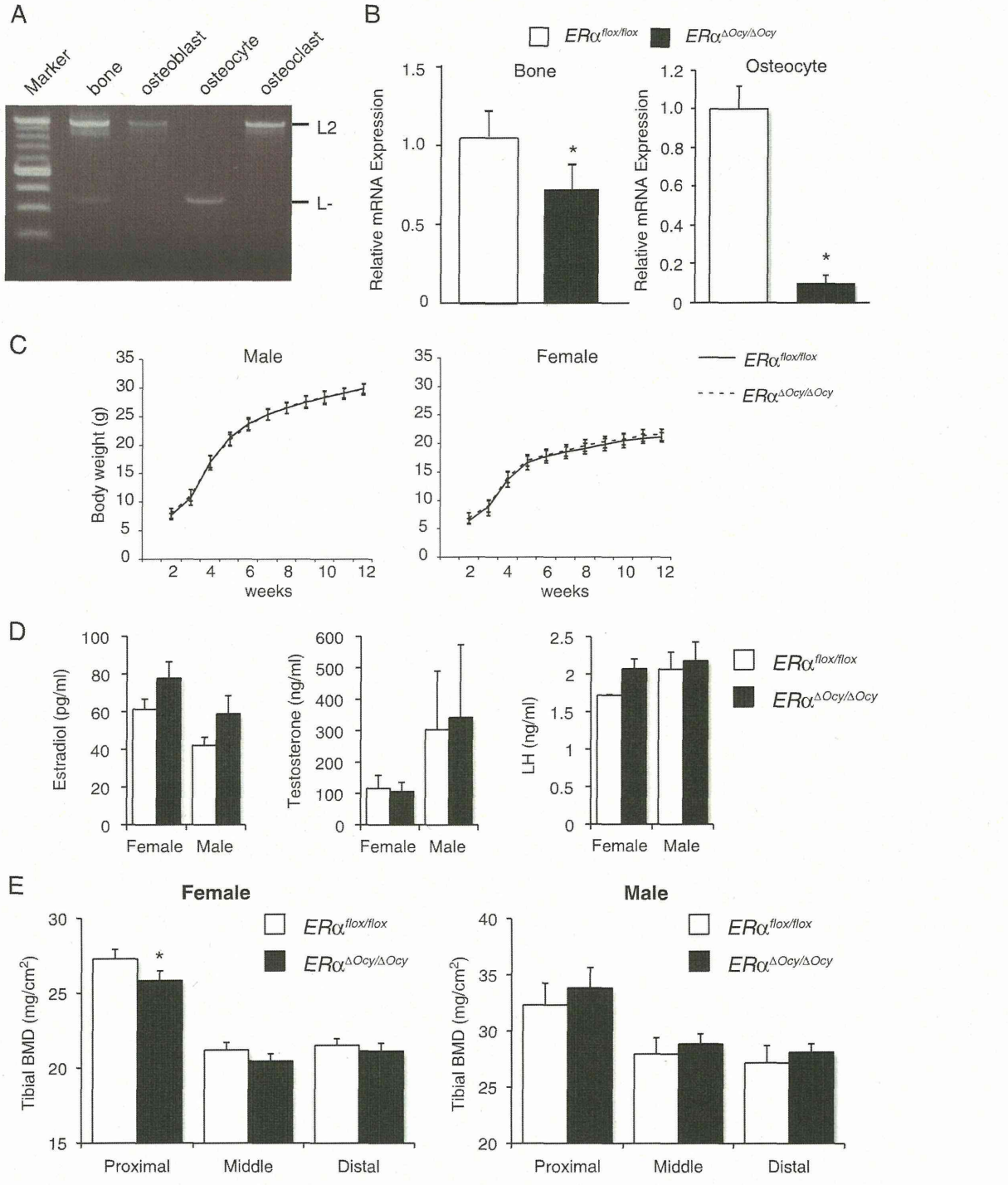

Fig. 1. Generation of mice with targeted deletion of ERα in osteocytes. (A) Deletion of ERα gene locus in osteocyte was detected by genome PCR in $ERα^{ΔOcy/ΔOcy}$. (B) mRNA levels of ERα from whole femurs (left panel) and isolated osteocytes (right panel) of $ERα^{flox/flox}$ and $ERα^{ΔOcy/ΔOcy}$ mice was evaluated by RT-qPCR. Data are represented as mean ± SEM (n = 3). (C) The growth curves of $ERα^{flox/flox}$ and $ERα^{ΔOcy/ΔOcy}$ mice. Data are represented as mean ± SEM (n = 7–10). (D) Serum hormone levels of 12-week-old $ERα^{flox/flox}$ and $ERα^{ΔOcy/ΔOcy}$ mice. Data are represented as mean ± SEM (n = 4–7). (E) BMD of 1/3 portion of longitudinal divisions of tibiae from 12-week-old $ERα^{flox/flox}$ and $ERα^{ΔOcy/ΔOcy}$ mice. Data are represented as mean ± SEM (Female n = 8, Male n = 7). * indicates $p < 0.05$.

Dmp1-GFP+; $ERα^{L2/L2}$ (*Dmp1-GFP*+; $ERα^{flox/flox}$) were generated by crossing *Dmp1-GFP*+; $Dmp1^{Tg/0}$; $ERα^{L2/+}$ and $ERα^{L2/L2}$. Calvariae obtained from approximately 10-day-old female *Dmp1-GFP*+; $ERα^{ΔOcy/ΔOcy}$ and *Dmp1-GFP*+; $ERα^{flox/flox}$ were treated with sequential enzymatic digestion and subjected to FACS. The percentage of GFP+ cells in fractions 4 to 6 was increased compared to that in fractions 2 to 4 (23.3% and 8.2%, respectively) (Fig. 4A). To determine if osteocytes were highly purified in this system, gene expression of cell-type specific marker genes in GFP+ cells (osteocytes) and GFP− cells (osteoblasts) was confirmed by RT-qPCR. As a result, the expression of Dmp1 (osteocyte marker